STUDY ON THE DIFFERENTIAL SCATTERING CROSS SECTION FOR NEUTRON-CARBON (n-^{12}C) NUCLEUS WITH EIKONAL APPROXIMATION

Hla Myat Thandar[1] and Khin Swe Myint[2]

Abstract

The purpose of this work is to predict the differential cross sections of neutron-carbon (n-^{12}C) nucleus in the frame work of Eikonal approximation. The differential cross sections of neutron-carbon nucleus are calculated by using Wood-Saxon potential. The projectile neutron kinetic energy ranged from 65 MeV to 95 MeV by increasing 10 MeV while the scattering angle varied 0° to 30°. The calculated results are in good agreement with the experimental results for energies, 65 MeV and 75 MeV. They are quite different for 85 MeV and 95 MeV.

Keywords: differential cross section, Eikonal approximation method, Wood-Saxon potential

Introduction

Scattering theory is a framework for studying and understanding the scattering of waves and particles. Understanding the nucleon-nucleus interaction has been one of the long term goals of nuclear physics. The nature of forces between particles can be studied from the scattering experiments. The interaction between two nucleons is basis for all of the nuclear physics. Approximations play a very important role in the understanding of processes that cannot be solved exactly. The Born approximation in quantum mechanics is an example of an approximation that has been extensively used for studying low energy processes.

There have been many measurements of proton-nucleus scattering, but few of neutron scattering at 65 MeV to 95 MeV energies. Those of Hjort *et al.* 65 MeV (Hjort E.L. et al., (1994)), Salmon at 96 MeV (Salmon G.L., (1960)), and from the Uppsala facility ((Klug J. et al., (2002), Klug J. et al., (2003), Klug J. et al., (2003)), also at 96 MeV are the most recent. In the 1950's and 1960's, when high energy physics was ascending towards its peak, it was realized among the high energy physicists of that time the Born approximation is not a valid approximation for studying processes involving high energies. This period in fact was the golden age in the development of the Eikonal approximation. From approximation methods, we can obtain differential scattering cross section.

Differential Cross Section and Electric Form Factors

If the colliding particles possess extended structure, the cross section must be modified. It must take into account only the spatial distribution of the target particle if the incident particles are leptons. For simplicity, we shall assume here that the target particle possesses a spherically symmetric density distribution. The cross section for scattering of electrons (Nakano T. et al., (1953)) from such a target is of the form.

$$\frac{d\sigma}{d\Omega} = \left(\frac{d\sigma}{d\Omega}\right)_{point} \left|F(q^2)\right|^2 \tag{1}$$

[1.] Dr, Lecturer, Department of Physics, University of Mandalay, Myanmar
[2.] Dr, Emeritus Professor, Department of Physics, University of Mandalay, Myanmar

The multiplicative factor $F(q^2)$ is called the Form Factor, and

$$q^2 = (p - p')^2$$

is the square of the momentum transfer, p is the momentum of incident particle and p' is the momentum of scattered particle.

Form Factors play an increasingly important role in nuclear physics because they are the most convenient link between experimental observation and theoretical analysis. Equation (1) expresses the fact that the Form factor is the direct result of a measurement. To discuss the theoretical side, consider a system that can be described by a wave function $\Psi(r)$, which in turn can be found as the solution of a Schrodinger equation. For an object of charge Q, the charge density can be written as Q $\rho(r)$, where $\rho(r)$ is normalized probability density, $\int d^3r\rho(r) = 1$. It is well known that the form factor can be written as the Fourier transform of the probability density

$$F(q^2) = \int d^3r\rho(r)e^{\frac{iq.r}{\hbar}} \tag{2}$$

The Form Factor at zero momentum transfer, F(0), is usually normalized to be 1 for a charged particle; however for a neutral one F(0)=0. The chain linking experimentally observed cross section to the theoretical point of departure can thus be sketched as follows:

Experiment Comparison Theory

$$\frac{d\sigma}{d\Omega} \rightarrow \left|F(q^2)\right| \Leftrightarrow F(q^2) \leftarrow \rho(r) \leftarrow \psi(r) \leftarrow \text{Schrodingrequation}$$

Calculation of The Scattering Amplitude by Using Eikonal Approximation

In theoretical physics, the eikonal approximation is an approximative method useful in wave scattering equations which occur in optics, seismology, quantum mechanics, quantum electrodynamics, and partial wave expansion.

The main advantage that the eikonal approximation offers is that the equations reduce to a differential equation in a single variable. This reduction into a single variable is the result of the straight line approximation or the eikonal approximation which allows us to choose the straight line as a special direction (Zamrun M. et al., (2013)).

At E>> V, the semiclassical path concept becomes applicable and we replace exact wave function ψ^+ by the semiclassical wave function,

$$\psi^+ \sim \; e^{iS(x)/\hbar} \tag{1}$$

The time independent Schrodinger equation is

$$H\left|\psi^+\right\rangle = E\left|\psi^+\right\rangle_{pp}$$

$$(H_0 + V)\left|\psi^+\right\rangle = E\left|\psi^+\right\rangle$$

$$\left(\frac{-\hbar^2}{2m}\nabla^2 + V\right)\left|\psi^+\right\rangle = E\left|\psi^+\right\rangle \tag{2}$$

Where $$H_0 = \frac{-\hbar^2}{2m}$$

Substitute equation (1) into equation (2) and ∇^2 for one dimension,

Equation (2) becomes

$$\frac{-\hbar^2}{2m}\frac{d^2}{dx^2}e^{iS(x)/\hbar} + Ve^{iS(x)/\hbar} = Ee^{iS(x)/\hbar} \quad (3)$$

From equation (3)

$$\frac{d^2}{dx^2}e^{iS(x)/\hbar} = \frac{d}{dx}\left[e^{iS(x)/\hbar} \circ \frac{i}{\hbar} \circ \frac{d}{dx}S(x)\right] = \frac{-1}{\hbar^2}e^{iS(x)/\hbar}\left(\frac{dS(x)}{dx}\right)^2 + \frac{i}{\hbar}e^{iS(x)/\hbar}\frac{d^2S(x)}{dx^2} \quad (4)$$

Substitute equation (4) into equation (3), Equation (3) becomes

$$\frac{1}{2m}e^{iS(x)/\hbar}\left(\frac{dS(x)}{dx}\right)^2 - \frac{i\hbar}{2m}e^{iS(x)/\hbar}\frac{d^2S(x)}{dx^2} + Ve^{iS(x)/\hbar} = Ee^{iS(x)/\hbar}$$

where $\hbar$ is very small,

$$\frac{1}{2m}\left(\frac{dS(x)}{dx}\right)^2 + V = \frac{\hbar^2k^2}{2m} \quad (5)$$

where $$E=\frac{\hbar^2k^2}{2m}$$

Equation (5) for 3 dimension,

$$\frac{(\nabla S)^2}{2m} + V = \frac{\hbar^2k^2}{2m} \quad (6)$$

This leads to the Hamilton-Jacobi equation for S

By equation (5) for one dimension,

$$\frac{1}{\hbar}\left(\frac{dS(x)}{dx}\right) = \sqrt{k^2 - \frac{2m}{\hbar^2}V(x)}$$

By integrating the above equation,

$$\frac{1}{\hbar}\int\frac{dS(x)}{dx}dx = \int\left(k^2 - \frac{2m}{\hbar^2}V(x)dx\right)^{1/2} + \text{constant}$$

$$\frac{S(x)}{\hbar} = \int\left(k^2 - \frac{2m}{\hbar^2}V(x)dx\right)^{1/2} + \text{constant} \quad (7)$$

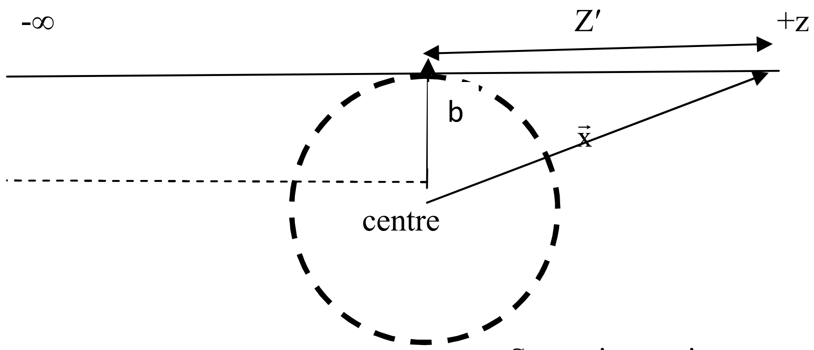

Scattering region

Consider the situation depicted in Fig, where the straight line trajectory is along the z-direction, |x|=r and |b|=b is the impact parameter.

Therefore equation (7) becomes,

$$\frac{S}{\hbar} = \int_{-\infty}^{z}\left(k^2 - \frac{2m}{\hbar^2}V\left(\sqrt{b^2+z'^2}\right)\right)^{1/2} dz' + \text{ constant} \qquad (8)$$

When $\quad V=0,\ e^{ikz} = e^{iS/\hbar}$

$$\therefore kz = S/\hbar$$

Equation (8) becomes

$$kz = \int_{-\infty}^{z} kdz' + \text{ constant}$$

$$\text{constant}= kz - \int_{-\infty}^{z} kdz'$$

Substitute in equation (8)

$$\frac{S}{\hbar} == \int_{-\infty}^{z}\left(k\left[1-\frac{2m}{\hbar^2k^2}V\left(\sqrt{b^2+z'^2}\right)\right]^{1/2} - k\right)dz' + kz \qquad (9)$$

By using power series,

$$(1-x)^n = 1 - nx + \frac{n(n-1)}{2!}x^2 - \ldots\ldots\ldots\ldots\ldots$$

$$\left(1-\frac{2m}{\hbar^2k^2}V\right)^{1/2} = 1 - \frac{1}{2}\frac{2m}{\hbar^2k^2}V + \ldots\ldots\ldots\ldots$$

$$\frac{S}{\hbar} == kz - \frac{m}{\hbar^2k}\int_{-\infty}^{z} V\left(\sqrt{b^2+z'^2}\right)dz'$$

$$\psi^+(X) = \psi^+(b + z\hat{z})$$

$$= e^{i\left[kz - \frac{m}{\hbar^2k}\int_{-\infty}^{z} V\left(\sqrt{b^2+z'^2}\right)dz'\right]}$$

$$= \exp(ikz) \circ \exp\left(-\frac{im}{\hbar^2 k} \int_{-\infty}^{z} V\left(\sqrt{b^2 + z'^2}\right) dz' \right) \tag{10}$$

The form factor is

$$f(k',k) = -\frac{1}{4\pi}\frac{2m}{\hbar^2}(2\pi)^3 \int d^3x' \frac{e^{-ik'.x'}}{(2\pi)^{3/2}} V(x') \langle X' | \psi^+ \rangle \tag{11}$$

$$\langle X' | \psi^+ \rangle = \frac{e^{iS(x)/\hbar}}{(2\pi)^{3/2}}$$

$$= \frac{1}{(2\pi)^{3/2}} e^{ikz'} e^{\frac{-im}{\hbar^2 k}\int_{-\infty}^{z} V\left(\sqrt{b^2+z''^2}\right)dz''}$$

Equation (11) becomes

$$f(k',k) = \frac{-1}{4\pi}\frac{2m}{\hbar^2}(2\pi)^3 \int d^3x' \frac{e^{-ik'..x'}}{(2\pi)^{3/2}} V(x') \langle X' | \psi^+ \rangle$$

$$= \frac{-1}{4\pi}\frac{2m}{\hbar^2} \int d^3x' e^{i(k-k')x'} V\left(\sqrt{b^2 + z'^2}\right) e^{\frac{-im}{\hbar^2 k}\int_{-\infty}^{z} V\left(\sqrt{b^2+z''^2}\right)dz''}$$

For cylindrical coordinate

$$d^3x' = bdb\, d\varphi_b\, dz'$$

$$(k-k')x' = (k-k').(b + z\hat{z})$$

$$(k-k')x' = (k-k').b + (k-k')z\hat{z}$$

$$= kb - k'b + (k-k')z\hat{z} \quad = -k'b$$

$$k'.b = (k\sin\theta\hat{x} + k\cos\theta\hat{y}).(b\cos\varphi_b\hat{x} + b\sin\varphi_b\hat{y})$$

$$= kb\sin\theta\cos\phi_b = kb\theta\cos\phi_b$$

The expression for f(k, k) becomes

$$f(k',k) = \frac{-1}{4\pi}\frac{2m}{\hbar^2}\int_0^{\infty} bdb \int_0^{2\pi} d\varphi_b e^{-ikb\theta kb\theta c_b} \int_{-\infty}^{\infty} dz' V \exp\left[\frac{-im}{\hbar^2 k}\int_{-\infty}^{z} Vdz''\right] \tag{12}$$

$$\int_0^{2\pi} d\varphi_b e^{-ikb\theta\cos\varphi_b} = 2\pi J_0(kb\theta) \quad \text{(bessel function)}$$

$$\int_{-\infty}^{\infty} dz' V \exp\left[\frac{-im}{\hbar^2 k}\int_{-\infty}^{z} Vdz''\right] = V\int_{-\infty}^{\infty} dz' \exp\left[\frac{-imV}{\hbar^2 k}\int_{-\infty}^{z} dz''\right]$$

$$= \frac{i\hbar^2 k}{m}\left[\exp\left(\frac{-im}{\hbar^2 k}\int_{-\infty}^{\infty} Vdz''\right) - 1\right] \tag{13}$$

By substituting equation (13) into equation (12),

$$f(k',k)=\frac{-1}{4\pi}\frac{2m}{\hbar^2}\int_0^\infty bdb2\pi\, J_0\left(kb\theta\right)\frac{i\hbar^2 k}{m}\left[\exp\left(\frac{-im}{\hbar^2 k}\int_{-\infty}^{\infty} Vdz''\right)-1\right]$$

$$=-ik\int_0^\infty bdbJ_0\left(kb\theta\right)\left[\exp\left(\frac{-im}{\hbar^2 k}\int_{-\infty}^{\infty} Vdz''\right)-1\right]$$

where $\Delta b=\dfrac{-m}{2k\hbar^2}\displaystyle\int_{-\infty}^{\infty} V\left(\sqrt{b^2+z''^2}\right)dz''$

The scattering amplitude is

$$f(k',k)=-ik\int_0^\infty bdbJ_0\left(kb\theta\right)\left[e^{2i\Delta b}-1\right] \qquad (14)$$

$$\boxed{\frac{d\sigma}{d\Omega}=\left|f(k',k)\right|^2=\left|f\left(\theta\right)\right|^2} \qquad (15)$$

Woods-Saxon Potential

Nuclear potential of the Woods-Saxon form, which is described by the potential depth V_0, the radius parameter r_0 and the diffuseness parameter *a*, is widely used in the analyses of nuclear collisions. The diffuseness parameter determines the characteristic at the surface region of the nuclear potential.

$$V(r)=\frac{V_0}{1-\exp\left(\dfrac{r-R}{a}\right)}$$

where V_0 = 50 MeV (potential well depth)

$R = r_0 A^{1/3}$ (nuclear radius)

r_0 = 1.25 fm (the radius parameter)

a = 0.5 fm (the surface diffuseness parameter)

Results and Discussions

Differential scattering cross sections of neutron-carbon nucleus (n-^{12}C) are calculated by using Wood-Saxon potential. In this calculation, the energies of neutron ranged from 65 MeV to 95 MeV by increasing 10 MeV while the scattering angle varied 0° to 30°. To investigate differential scattering cross sections of the n-^{12}C nucleus, Eikonal approximation method is used. It is found that the smaller the scattering angle, the larger the differential scattering cross section. Moreover, the larger the energy of the neutron, the larger the differential scattering cross section is. The calculated results of differential scattering cross sections are in good agreement with the experimental results for energies, 65 MeV and 75 MeV. But they are quite different with the experimental results for 85 MeV and 95 MeV. Moreover, they are slightly different at large angles. But the features of the calculated results and the experimental results are similar. They are shown in Figure (1) to Figure (5).

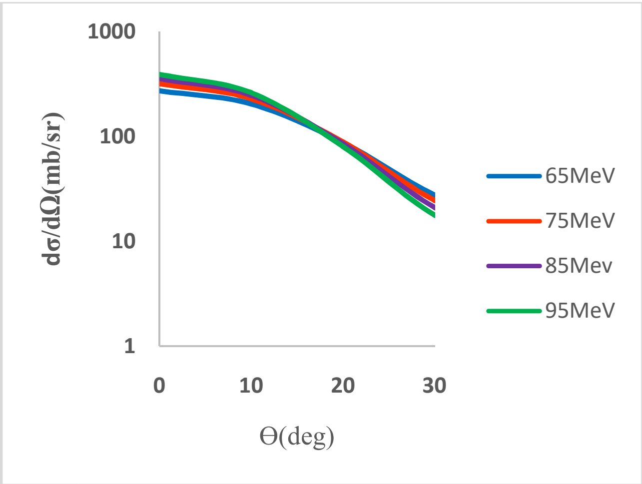

Figure 1 Our calculated results of differential scattering cross sections for 65 MeV to 95 MeV

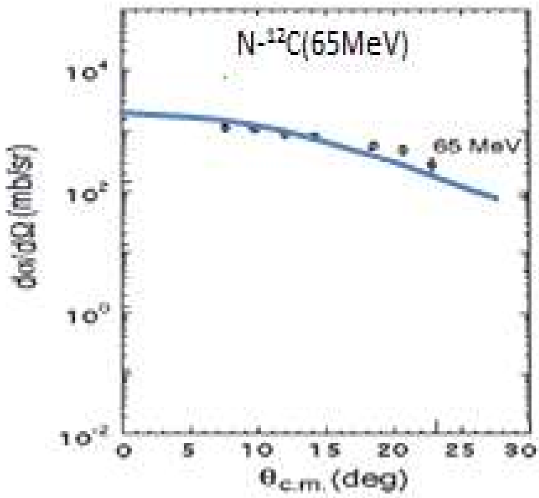

Figure 2 Comparison between experimental result and our calculated result of differential scattering cross section for 65 MeV

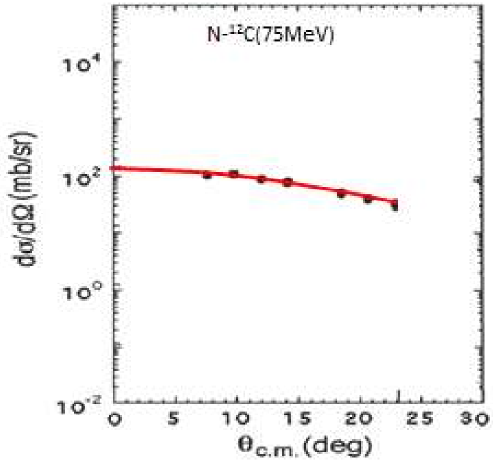

Figure 3 Comparison between experimental result and our calculated result of differential scattering cross section for 75 MeV

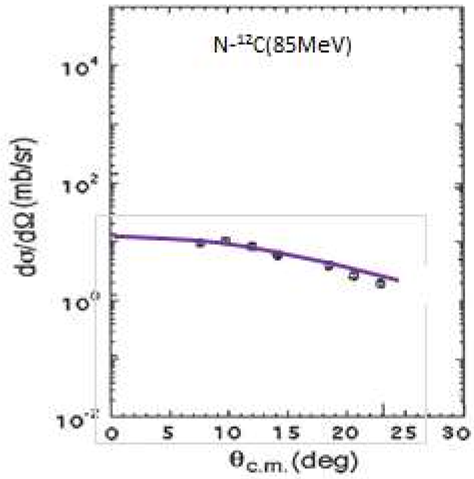

Figure 4 Comparison between experimental result and our calculated result of differential scattering cross section for 85 MeV

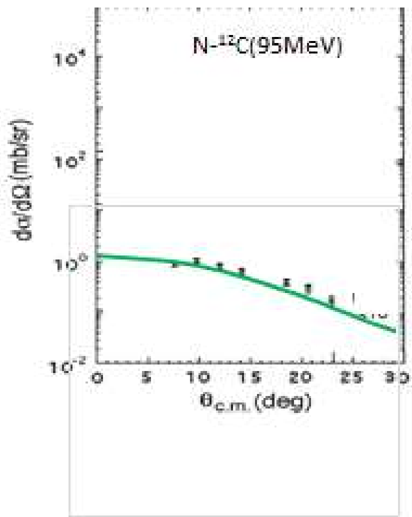

Figure 5 Comparison between experimental result and our calculated result of differential scattering cross section for 95 MeV

Acknowledgements

I would like to specially thank to my supervisor, Dr Khin Swe Myint, Emeritus Professor, Rector (Rt.d), University of Mandalay, for her invaluable advices and enthusiastic guidance throughout this work.

I do thank Dr Lei Lei Win, Professor and Head of Physics Department, University of Mandalay, for her encouragement and permission.

References

Hjort E.L. et al., (1994). Phys. Rev. C **50** 275.

Klug J. et al., (2002). Phys. Res. A **489** 282.

Klug J. et al., (2003). Phys. Rev. C **67** 031601(R).

Klug J. et al., (2003). Phys. Rev. C **68** 064605.

Nakano T. et al., (1953). Phys. Rev. **92** 833.

Salmon G.L., (1960). Nucl. Phys. **21** 15.

Zamrun M. et al., (2013). Phys. Rev. **C 87** 024611.